

Modulating LiFi for Dual Operation in the Visible and Infrared Spectra

Dayrene Frometa Fonseca^{a,b,*}, Muhammad Sarmad Mir^b, Sergio Iglesias de Frutos^{a,c}, Borja Genoves Guzman^d, Domenico Giustiniano^a

^aIMDEA Networks Institute, Leganes, 28918, Madrid, Spain

^bUniversidad Carlos III de Madrid, Leganes, 28911, Madrid, Spain

^cUniversidad Politecnica de Madrid, Madrid, 28040, Spain

^dUniversity of Virginia, Charlottesville, 22904, Virginia, USA

Abstract

Light-Fidelity (LiFi) has emerged in the last few years as a promising technology for alleviating the stringent demand for wireless data services. Prior works have considered LiFi operating either in the visible light or infrared spectrum. Each spectrum band has its own advantages: visible light allows leveraging existing infrastructure for communication, while infrared is not affected by light dimming. In this work, we propose a modulation scheme that retains the benefits of both bands, introducing a simple, low-cost, yet efficient dimming solution for LiFi networks. We compare the performance of the proposed dimming scheme with both the digital and analog dimming techniques traditionally used in LiFi systems. Simulation results show that our dimming solution offers better communication and illumination performance than previous proposals, providing larger signal-to-noise ratio, spectral efficiency, and a full and fine-grained dimming range. Finally, we prototype our solution by designing an extended version of the OpenVLC 1.3 platform, and we experimentally show its robust communication performance under different dimming conditions. We make the implemented system publicly available to the research community.

Keywords:

Dimming, Infrared (IR) Spectrum, LiFi, Visible Light (VL) Spectrum

1. Introduction

In the past few years, there has been an increasing interest in the research, development, and commercialization of Light-Fidelity (LiFi). LiFi is considered a promising solution to alleviate the Radio Frequency (RF) spectrum crunch problem in 6G networks and to serve Internet of Things (IoT) devices [1]. LiFi systems operating in the *visible light (VL) spectrum* (wavelengths between 380 nm and 780 nm) reuse the existing Light Emitting Diode (LED)-based illumination infrastructure, retrofitted for communication purposes. This approach has two advantages: it significantly reduces the infrastructure and deployment costs of LiFi solutions and greatly reduces the energy required for communication, as illumination consumes much higher energy than communication [2]. However, one mandatory requirement of LiFi communication systems operating in the VL spectrum is to provide dimming support [3], adjusting the brightness of light bulbs according to the users' comfort without decreasing the communication performance.

Earlier light communication standards, i.e., IEEE 802.15.7-2011 [3] and IEEE 802.15.13 [4], use the VL spectrum to target short-range optical communications and multi-gigabit optical

wireless communication, respectively. Instead, the most recent IEEE 802.11 TGbb standard [5] focuses on achieving high data rates but ensuring the rapid market adoption of LiFi technology. To this end, the standardization effort has focused on enabling existing chipsets, such as WiFi, to work in the *infrared (IR) spectrum* band. According to the IEEE 802.11 TGbb, the up-link and downlink operation of LiFi systems in the IR spectrum is mandatory with wavelengths between 800 nm and 1000 nm. The advantage of this approach is that dimming does not need to be taken into account in the IR band, which allows for easing the commercialization of LiFi solutions. However, it results in losing one of the aforementioned advantages of LiFi systems, which is to retrofit existing lighting infrastructure for communication.

Heterogeneous networks (HetNets) have been proposed to optimize network efficiency and throughput [6]. In that sense, recent hybrid RF-LiFi systems can complement each other in alleviating problems such as traffic congestion in RF systems or LiFi blockage [7]. However, LiFi systems can barely complement RF systems if the dimming problem is not addressed, which is one of the most limiting issues of LiFi technology when operating in the visible light band. In this work, we focus on hybrid optical systems to provide good communication performance even under extreme dimming conditions. Specifically, we envision that future LiFi systems will operate in *both* VL and IR spectra, retaining the advantages of both bands for robust communication and precise dimming control. From a

*Corresponding author.

Email addresses: dayrene.frometa@imdea.org (Dayrene Frometa Fonseca), sarmadmir2003@gmail.com (Muhammad Sarmad Mir), sergio.iglesias.defrutos@alumnos.upm.es (Sergio Iglesias de Frutos), rrc3wc@virginia.edu (Borja Genoves Guzman), domenico.giustiniano@imdea.org (Domenico Giustiniano)

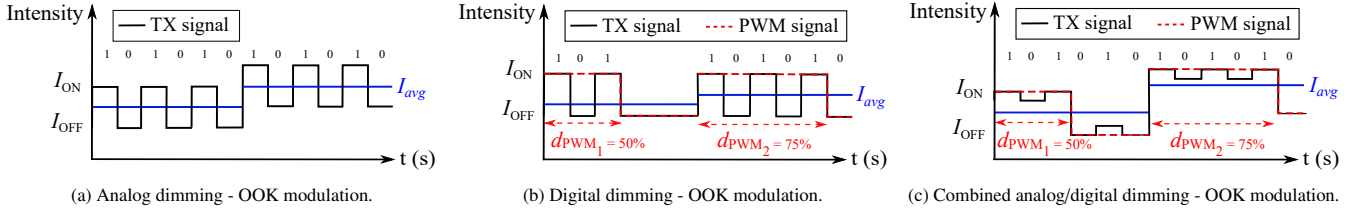


Figure 1: State-of-the-art OOK dimming techniques.

technological standpoint, LED bulbs are typically composed of multiple small Surface Mounted Device (SMD) LEDs. In the future, some of these SMDs LEDs could be operating in the VL band, and others in the IR one. Therefore, it would be simple to extend the functionalities of LED bulbs to operate in both spectra. Besides, some works have demonstrated the feasibility, from a techno-economic perspective, of adopting a joint VL and IR system for communication [8]. Our solution takes also advantage of the fact that the responsivity of typical photosensitive devices covers both VL and IR spectra, and thus *no changes are required at the optical receiver*. However, operating in both VL and IR spectra requires the design of new modulation schemes that efficiently combine the transmissions in both bands, while taking care of dimming in the VL one, as we address in this paper.

The *trivial solution* would be to dedicate VL LEDs for illumination and IR LEDs for communication, but this would increase the overall energy consumption, as it will be shown in the results section of this paper. Therefore, a different approach is needed to cover this larger spectrum. Unlike previous work that proposed complex techniques for implementing dimming in LiFi [9], in this paper we propose a *low-power modulation scheme* based on On-Off-Keying (OOK) and Pulse Width Modulation (PWM) that can operate in *both the VL and IR bands*, for fulfilling *both illumination standards and required communication performance*. Due to its simplicity, our modulation scheme can be extended to multiple low-end and energy-constrained systems, such as IoT devices for applications in smart homes, offices, and Industry 4.0. We have experimentally validated our proposal by designing a Printed Circuit Board (PCB) that is an extension cape for the PocketBeagle [10], and the firmware required to control it. This is an extended and renewed version of the design presented in the past by the same authors [11], and we make the hardware and software design publicly available¹. Compared to the previous published works [11, 12], the main contributions of this paper are summarized as follows:

- We highlight the challenges of providing a reliable dimming technique for LiFi systems.
- We present a detailed mathematical analysis of the proposed solution, which allows extending the results to a multi-cell scenario. We study these new scenarios and present simulation results for the received signal-to-noise

power ratio (SNR) and the average illuminance under different dimming levels.

- We also improve the prototype used for experimental evaluation in [11], now implementing it with the PocketBeagle [10]. This reduces the PCB size, cost, and power consumption, which makes our prototype be more appealing for reproducibility. Unlike state-of-the-art OpenVLC-based papers [1], for the first time, this work provides the OpenVLC platform with dimming functionality.

The remainder of this paper is organized as follows. Section 2 and Section 3 summarize the state of the art on LiFi dimming techniques and the challenges addressed in this work, respectively. Section 4 details the proposed dimming scheme, while Section 5 and Section 6 describe the simulation results and experimental evaluation, respectively. Finally, Section 7 details the main applications of our system, and conclusions are drawn in Section 8.

2. Related Work

Existing techniques to adjust the brightness of an LED are classified into *analog dimming* and *digital dimming*. The former consists of decreasing the radiated optical flux of the LED by adjusting the amplitude of the forward current through it, while the latter is based on a digitally modulated pulse train whose duty cycle (d_{PWM}) determines the dimming level (i.e., a PWM signal) [13]. In the past years, these dimming techniques have been combined in many different ways with existing modulation schemes to convey data while providing dimming control in LiFi systems. Figure 1 depicts examples of the combination of analog and digital dimming techniques with OOK modulation, though any other modulation scheme can be employed.

Analog dimming with OOK, depicted in Fig. 1a, ensures low computational complexity and simple implementation, but directly changing the forward current through the LED alters the emitted wavelength of the light [13]. Moreover, the increase and decrease of the DC bias may cause degradation of the usable dynamic range, which decreases the spectral efficiency [14]. *Digital dimming* with OOK, represented in Fig. 1b, keeps the current level constant at the biasing point of the LED, and manages the dimming level with the duty cycle of a PWM signal [9]. Although this technique avoids the chromaticity shifts introduced by analog dimming, it still shows limitations in terms of achievable data rate because data is transmitted only while the PWM signal is ‘ON’. Different dimming techniques

¹https://github.com/openvlc/OpenVLC/tree/master/OpenVLC_VL_IR

combining both *analog and digital dimming* with existing modulation schemes have been proposed to solve the limitations mentioned above, as the one depicted in Fig. 1c where the amplitude of the signal dedicated to communication keeps constant, but its DC-bias changes according to the required dimming level [15].

Despite the research efforts in this area, most of the existing dimming proposals for LiFi systems present the following drawbacks: (i) limited dimming precision; (ii) constrained dimming range, being bounded by the maximum and minimum configurable light intensities (i.e., I_{ON} and I_{OFF} in Fig. 1); (iii) increased complexity when trying to balance communication performance and illumination [16]; and (iv) poor communication performance under high dimming conditions [17]. Moreover, most of the current solutions can only be applied to specific scenarios, such as the subcarrier-index-modulation-based dimming approach that can only be used with specific multi-carrier modulation schemes [18], or the spatial dimming proposal that relies on multi-LED systems [19]. Finally, most of the existing proposals have not been experimentally tested.

3. Challenges

In this section, we discuss the challenges faced to provide a reliable dimming technique in LiFi systems and how we solve them.

Wide-range, precise and flexible dimming. Two desirable features of dimming solutions for LiFi systems are: (i) to provide a wide dimming range, i.e., the ability to offer both sufficiently high and low illumination conditions, and (ii) to adjust the dimming level with high precision and flexibility. However, providing such features has proven to be challenging, as the LED light intensity, which determines the dimming level, is strictly tied to the LiFi communication performance. This limits the lower bound of the provided dimming level to ensure good performance of the LiFi link, and it also limits the communication range [13]. Likewise, providing high illumination conditions means, in most cases, adding a DC bias that reduces the system's power efficiency [14]. On the other hand, the problem of offering flexible and precise dimming control has been tackled with hybrid dimming approaches that adjust multiple resources simultaneously. For example, the work in [16] jointly changes the time-domain duty cycle and the intensity scaling factor, and authors in [18] use what they call frequency-domain and intensity-domain techniques to implement hybrid dimming control. However, these two-dimensional adjustments duplicate the implementation complexity.

Joint communication and illumination performance. As shown in Fig. 1, existing dimming techniques fail to provide a well-balanced joint communication and illumination performance. The analog dimming approaches decrease the intensity of the LED light to lower the illumination conditions [13], and the digital dimming approaches include a compensation time where no data is transmitted [9], which degrade both the communication performance by lowering the achievable range and the data rate.

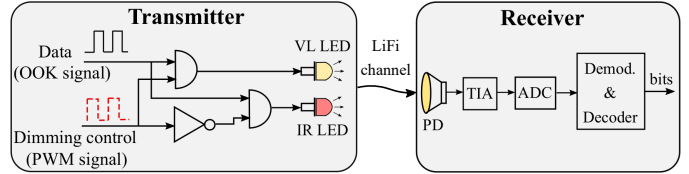


Figure 2: Block diagram of the proposed LiFi system.

Table 1: Digital signals fed to the VL and IR LEDs after logic gates.

OOK signal	PWM signal	VL LED	IR LED
0	0	0	0
1	0	0	1
1	1	1	0
0	1	0	0

Our solution. We solve the joint communication and illumination issue with a dimming approach that combines transmissions in the IR and VL bands. Specifically, we control the illumination conditions by means of a duty-cycle-based technique that determines the time transmitting on each band. By doing so, we do not damage the communication performance during dimming, being able to provide extremely low illumination conditions (even zero) while keeping a reliable LiFi link. To ensure precise and flexible dimming control, we rely on a PWM signal to manage the duty cycle. Details on the proposed dimming scheme are given in the following section.

4. Proposed dimming scheme

Figure 2 presents the block diagram of our proposed LiFi transmitter and receiver for dual operation in the VL and IR spectra. As can be observed, from two input signals (i.e., OOK signal and PWM signal) and after some logic gates, we determine the signals transmitted by the VL and IR LEDs. Table 1 shows the results of the proposed logic gates combination to enable each LED and to have control over the dimming level in the VL band. When a bit ‘1’ is transmitted, at least one LED must be ‘ON’, either the VL or the IR one, depending on the PWM signal that controls the illuminance (VL emitted). To provide more details, Fig. 3 represents some examples of the signals emitted by each LED for different dimming levels. \bar{P}_{VL} and \bar{P}_{opt} denote the average VL optical power emitted for each dimming case and the total average optical power (VL+IR), respectively. As depicted, our modulation scheme combines OOK and PWM modulations for communication and dimming purposes, respectively. Specifically, as said before, when sending the OOK symbol ‘1’, the transmitter switches between the VL and IR bands following a PWM signal whose duty cycle (d_{PWM}) determines the provided dimming level. As shown in Fig. 3, when the PWM signal is ‘ON’, the transmitter operates on the VL band sending out a VL signal that contributes to illumination purposes. In turn, when the PWM signal is ‘OFF’, the sender works on the IR band generating an IR signal that contributes to dimming. In this way, the higher d_{PWM} , the lower the dimming level is.

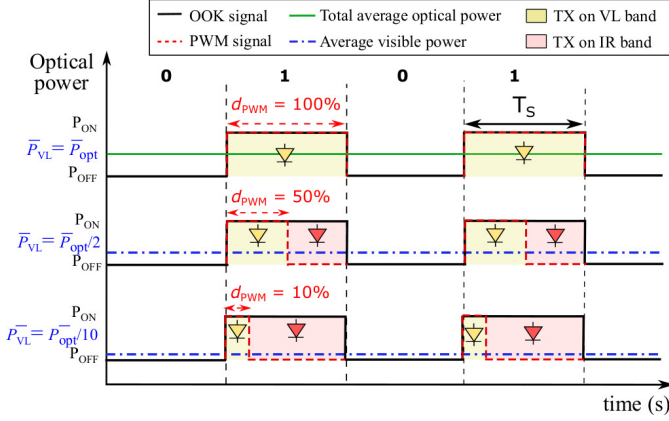


Figure 3: Proposed modulation scheme.

Note that the proposed technique can be extended to other modulation schemes by alternating between VL and IR LEDs. As examples, within the pulse-based modulation schemes we can implement a pulse position modulation (PPM) or a pulse-amplitude modulation (PAM) if the system requires a larger energy efficiency or spectral efficiency [20], respectively. We can also build a more robust system at the expense of a peak-to-average-power ratio (PAPR) and complexity increase by using any optical orthogonal frequency division multiplexing (O-OFDM) technique [20, 21]. However, in this paper we prefer to consider an OOK modulation scheme due to its simplicity and because it eases the understanding of our proposal.

In LiFi networks using the dimming scheme proposed here, any photodiode (PD) with sensitivity in both the VL and IR bands can be employed as receiver. If we look at the responsivity of photosensitive devices, as long as the power received at IR and VL bands are the same, we find that they provide better performance when operating in the IR band than in the VL one. This is represented in Fig. 4, which depicts the actual spectral responsivity of the ‘VTP4085H’ PD. The reason is that the energy of a photon is inversely proportional to its wavelength, and the quantum efficiency of a photosensitive device can be formulated as

$$QE(\lambda) = \frac{\eta_{PD}(\lambda)}{\lambda} \cdot (1240 \text{ W} \cdot \text{nm/A}), \quad (1)$$

where $\eta_{PD}(\lambda)$ is the responsivity at the wavelength λ measured in A/W. Thus, η_{PD} increases with λ , which is why IR wavelengths offer better responsivity than VL wavelengths. In this paper, we take advantage of this not only to implement a dimming technique that provides dimming ranges wider than traditional approaches, but also to ensure high-quality communication links even under extreme dimming conditions. As shown in Fig. 2, the signal reception process consists of a transimpedance amplifier (TIA), an analog-to-digital converter (ADC), a demodulator with a threshold to decide between bit ‘1’ and ‘0’, and a decoder. Note that the receiver follows a conventional design and that no modifications are required to operate with the modulation technique proposed in this paper.

From Fig. 3, it should also be noticed that the total optical power when operating in the VL and IR bands is exactly

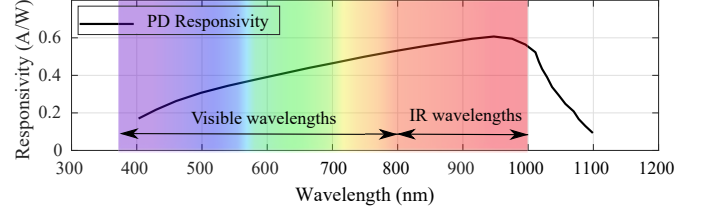


Figure 4: Responsivity of the ‘VTP4085H’ PD at the receiver.

the same, which is ensured by carefully adjusting the electrical/optical parameters of the LEDs, as explained later on. By doing so, we make the upper layers agnostic to the type of wavelength used, simplifying the design and avoiding a management layer to handle the used band at the receiver.

4.1. Analysis

Theoretically, the time-domain received signal can be formulated as

$$y(t) = \int_{\lambda} \eta_{PD}(\lambda) \cdot [x_{VL}(t, \lambda) + x_{IR}(t, \lambda)] \otimes h(t) d\lambda + n(t), \quad (2)$$

where $x_{VL}(t, \lambda)$ and $x_{IR}(t, \lambda)$ are the time-domain spectral signals emitted by the VL and IR LEDs, respectively, $h(t)$ is the time-domain channel and $n(t)$ corresponds to the time-domain receiver noise which follows a Gaussian distribution with mean and variance equal to zero and σ_{rx}^2 , respectively. Assuming that we operate at a frequency lower than the cut-off frequency of the front-end devices and that the signal power coming from reflections is negligible with respect to the signal power received from the line-of-sight path, the channel can be represented by

$$h(t) = h_{LOS} = \frac{A_{PD}(m+1)}{2\pi D^2} \cos^m(\phi) \cos(\psi), \quad (3)$$

where A_{PD} is the active area of the PD, $m = -1/\log_2(\cos(\phi_{1/2}))$ is the Lambertian index of LED, where $\phi_{1/2}$ is the half-power semi-angle, D denotes the Euclidean distance between the LED and the receiver, and ϕ and ψ are the irradiance and incidence angles, respectively. The SNR on the receiver side is computed as

$$SNR = \frac{P_{elec,rx}(d_{PWM})}{\sigma_{rx}^2}, \quad (4)$$

where $P_{elec,rx}$ is the received electrical power which depends on the duty cycle d_{PWM} represented in Fig. 3, and it is formulated according to the new modulation scheme as

$$P_{elec,rx}(d_{PWM}) = \left(\bar{P}_{opt} h_{LOS} \int_{\lambda} \eta_{PD}(\lambda) \cdot (d_{PWM} \hat{x}_{VL}(\lambda) + (1-d_{PWM}) \hat{x}_{IR}(\lambda)) d\lambda \right)^2, \quad (5)$$

where $\hat{x}_{VL}(\lambda)$ and $\hat{x}_{IR}(\lambda)$ are the normalized spectrum emitted by the VL and IR LEDs, respectively, i.e., $\int_{\lambda} \hat{x}_{IR}(\lambda) d\lambda = \int_{\lambda} \hat{x}_{VL}(\lambda) d\lambda = 1$. We assume that the optical transmit power when transmitting bit ‘0’ is $P_{OFF} = 0$. Note that bit ‘1’ and bit ‘0’ are sent with an equal probability. The emitted average

Table 2: Simulation parameters

Parameter	Value
VL LED model	XHP35B-00-0000-0D0HC40E7
IR LED model	LZ4-00R708
PD model	VTP4085H
P_{ON}	30 W
$\phi_{1/2}$	60°
F_s	10 MHz
T	300 K
R_L	50Ω

power is $\bar{P}_{opt} = P_{ON}/2$, where P_{ON} denotes the optical transmit power when transmitting bit '1'. If the radiation patterns of the VL and IR LEDs are different, to make a fair comparison between dimming levels, the emitted power at a specific irradiance angle must be the same, i.e., $P_{ON} \cdot (m+1) \cdot \cos^m(\phi)$ must be equal in both LEDs². The noise variance is composed by the noise power spectral densities of shot ($N_{0,s}$) and thermal ($N_{0,th}$) noises as

$$\begin{aligned} \sigma_{rx}^2 &= (N_{0,s} + N_{0,th}) \cdot F_s \\ &= \left(2q \sqrt{P_{elec,rx}} + \frac{4\kappa_B T}{R_L} \right) \cdot F_s, \end{aligned} \quad (6)$$

where F_s is the sampling frequency, q is the electrical electron charge, κ_B is the Boltzmann's constant, T is the absolute temperature at the receiver and R_L is the load at the receiver. For simplicity, we do not consider either user mobility, which would increase the probability of misalignment between transmitter and receiver [22], or sunlight, which would increase the noise power at the receiver according to eq. 6 [23]. All the modulation schemes under evaluation here will degrade equally under those new circumstances.

Finally, the theoretical spectral efficiency of an intensity modulation and direct detection (IM/DD) system can be formulated as [24]

$$SE = \frac{1}{2} \log_2 \left(1 + \frac{e}{2\pi} \cdot SNR \right). \quad (7)$$

We use the received illuminance as illumination metric in this paper. The corresponding received illuminance (measured in lux) can be formulated as

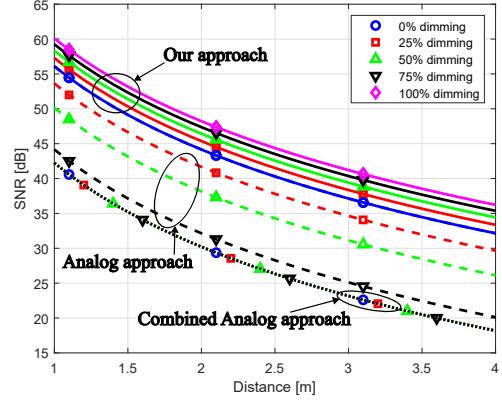
$$E_v(d_{PWM}) = \frac{\Phi_v(d_{PWM}) \cdot h_{LOS}}{A_{PD}}, \quad (8)$$

where Φ_v is the transmitted luminous flux (measured in lm) that is computed, considering only the visible emitted spectrum, as

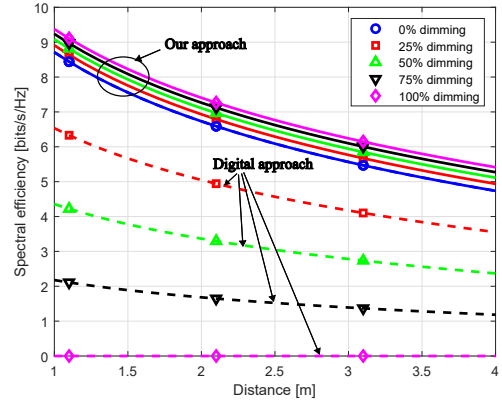
$$\Phi_v(d_{PWM}) = \bar{P}_{opt} \cdot 683.002 \int_{\lambda} d_{PWM} \cdot \hat{x}_{VL}(\lambda) V(\lambda) d\lambda, \quad (9)$$

where $V(\lambda)$ is the luminosity function representing the spectral sensitivity of the human eye.

²This will be solved when commercial light bulbs integrating VL and IR LEDs appear, since same coverage must be guaranteed regardless of the LED type.



(a) SNR against distance for our proposal, analog dimming and combined analog/digital dimming.



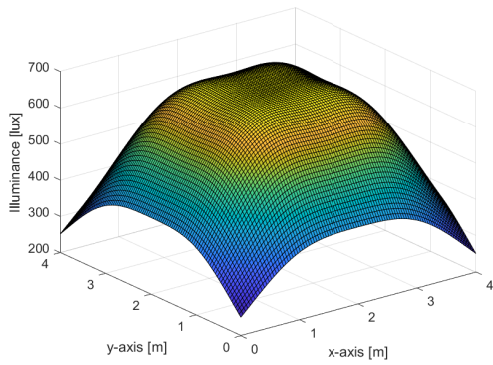
(b) Spectral efficiency against distance for our proposal and digital dimming.

Figure 5: Performance comparison between our proposal and state-of-the-art OOK dimming techniques.

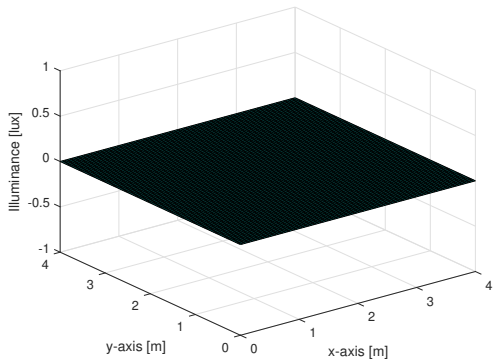
5. Simulation results

This section presents the simulation results where we compare our proposal with the state of the art, which includes the analog, digital, and combined digital-analog solutions depicted in Fig. 1. The simulation parameters are summarized in Table 2. We assume to use the actual XHP35B-00-0000-0D0HC40E7 and the LZ4-00R708 LED models for VL and IR transmission whose emitted optical spectral are obtained from their corresponding datasheets, and we employ the PD VTP4085H model as receiver, whose spectral responsivity is represented in Fig. 4. Then, we assume an emitted power of $P_{ON} = 30$ W when the LED is ON, a half-power semi-angle characterizing the LED radiation pattern of $\phi_{1/2} = 60^\circ$, a sampling frequency $F_s = 10$ MHz, an absolute temperature $T = 300$ K and a receiver load $R_L = 50 \Omega$. Note that, in practice, the configured emission power can be easily configured by setting the drive current and/or installing an array of LEDs.

Figure 5 shows results of SNR and spectral efficiency for different distances between transmitter and receiver. The transmitter and receiver are pointing at each other, then the irradiance and incident angles are $\phi = 0$ and $\psi = 0$, respectively. Overall, our proposal provides better communication performance

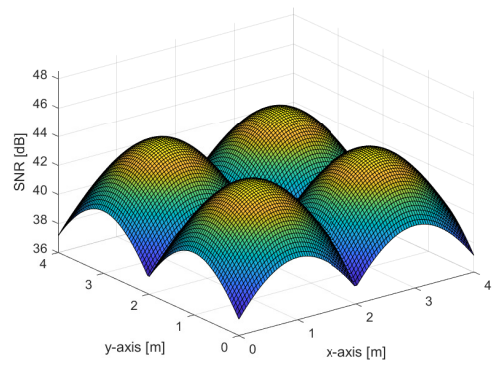


(a) 0% dimming.

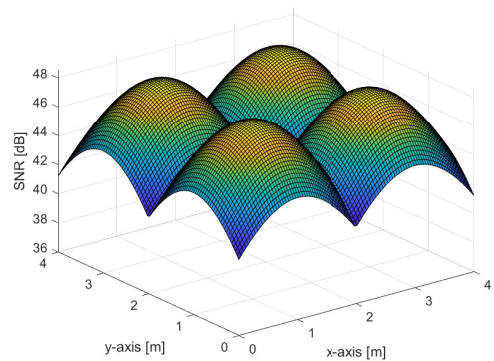


(b) 100% dimming.

Figure 6: Received illuminance for different dimming conditions when our proposal is implemented in a multi-cell scenario (4 transmitters) with room dimensions 4x4 m.



(a) 0% dimming.



(b) 100% dimming.

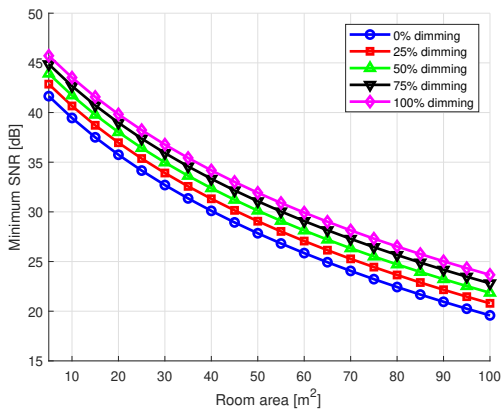
Figure 7: Received SNR for different dimming conditions when our proposal is implemented in a multi-cell scenario (4 transmitters) with room dimensions of 4x4 m.

for all dimming levels. As can be observed in Fig. 1, the analog approach reduces the amplitude of the transmitted signal to provide higher dimming levels, which has a dramatic impact on the SNR of the received signal. Differently, the digital approach stops the data transmission for higher dimming levels, significantly reducing the data rate. The combined analog/digital dimming approach keeps the SNR constant for any dimming level at the expense of a low amplitude of the signal, which also affects the SNR. These effects can be observed in Fig. 5. However, as shown in Fig. 3, our proposal relies on IR to complement the decreased visible light power and not damage the communication performance under dimming conditions. Then, unlike state-of-the-art techniques, our proposal provides better communication performance in terms of SNR and spectral efficiency at larger dimming levels due to the higher PD responsivity in the IR wavelengths. On the other hand, it should be noticed that our dimming technique offers a fine-grained dimming range with a high precision (from 0% to 100%). This is because, as shown in Fig. 3, the dimming level is managed by the duty cycle of a PWM signal.

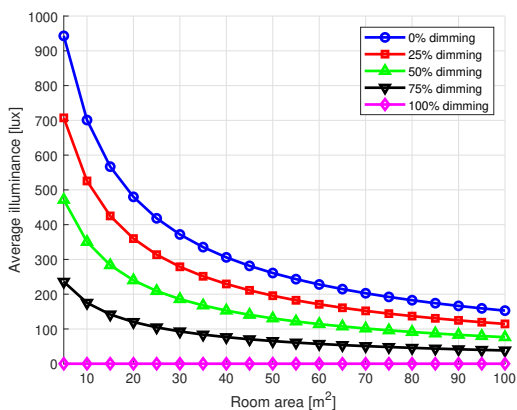
The different results obtained for each dimming level may be affected in a multi-cell scenario, both in terms of communication and illumination. Fig. 6 and Fig. 7 show the received illuminance and SNR results, respectively, obtained in a 4-

transmitter scenario with the LEDs deployed in a symmetric 2-by-2 lattice with x and y coordinates (1,1), (1,3), (3,1) and (3,3) meters. We assume that the desired signal comes from the nearest LED, that there is no cooperations from neighboring LEDs, and that each PD is oriented vertically looking upwards. The vertical distance between LED and PD is 2 m. As shown in Fig. 6, the average illuminance obtained with a 0% dimming level is 547 lux, while 0 lux of illuminance is obtained with a 100% dimming level. However, as depicted in Fig. 7, the SNR received at each location with 0% dimming is around 4 dB lower than the one received with 100% dimming. Note that these results are aligned with the ones presented in Fig. 5a, and they show how our system can work for different room sizes depending on the dimming level to be configured.

Then, in Fig. 8a and Fig. 8b, we show the minimum SNR and average illuminance obtained for different room sizes, always maintaining the symmetry in the LED distribution, i.e., the distance between LEDs is twice the distance between an LED and the room wall. Note in Fig. 8a that the minimum SNR decreases almost linearly with the room area, and the difference between the two extreme dimming levels is almost kept at 4 dB. This means that, when using a 100% dimming level, the room size can be larger for the same outage probability, defined as the probability for a user to have an SNR lower than cer-



(a) Minimum SNR obtained at different room sizes.



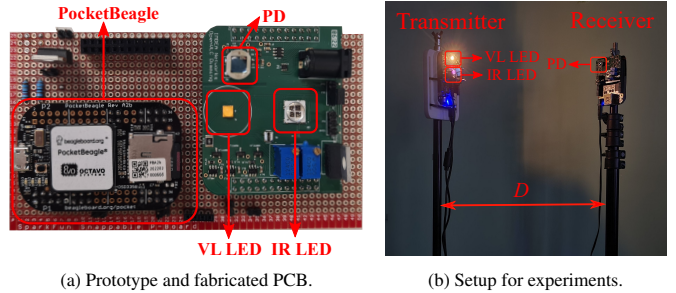
(b) Average illuminance obtained at different room sizes.

Figure 8: Communication and illumination performance of our proposal for different room sizes and dimming levels in a multi-cell scenario (4 transmitters).

tain threshold. However, as represented by Fig. 8b, the maximum room size may be limited by the average illuminance provided. According to illumination standards [25], the required average illuminance depends on the activity to be performed in such a room, but a minimum standard value of 500 lux is typically assumed. Thus, for such 500 lux value of average illuminance, our system can operate at a maximum room area of 20 m², which means a side length of around 4.5 m in a square room.

6. Implementation and Experimental Results

To confirm our simulation results, we implement the proposed transmitter and receiver in a PCB designed by ourselves. This PCB has been designed to be compatible with OpenVLC 1.3 [12]. Unlike other research-oriented LiFi platforms, OpenVLC is a low-end open source and open hardware platform for LiFi communication that offers TCP/IP capabilities. OpenVLC is based on the BeagleBone Black board (BBB) that provides Programmable Real-time Units (PRUs) and advantageously enables real-time operations with extreme time precision [1]. Our prototype and the experiment setup are shown in Fig. 9.



(a) Prototype and fabricated PCB.

(b) Setup for experiments.

Figure 9: Hardware and setup used for experiments.

Table 3: BeagleBone Black and PocketBeagle comparison

Parameter	BBB	PocketBeagle
Size [mm ²]	86.36 x 53.34	35.56 x 56.89
Power consumption [W]	10	1.25
Cost [€]	50	35
Storage	4GB eMMC Flash	8MB SPI Flash
Number of pins	92	72
Number of PRUs	2	2

6.1. Hardware and firmware implementation

OpenVLC 1.3 was initially designed to be powered and controlled by the BeagleBone Black [12, 26]. However, we found that the PocketBeagle [10] is an excellent alternative to minimize the control board's size, power consumption, and cost, facilitating its integration with commercial LED lamps and enabling its use in real applications that require dense LiFi deployments. As shown in Table 3, by adopting the PocketBeagle, we can reduce the size, power consumption, and cost of the control board in 56%, 87.5%, and 30%, respectively, compared to the BBB. Also, it should be noticed that despite the size and price reduction, the PocketBeagle keeps the required features to implement all the functionalities of our system, i.e., a sufficient number of pins, storage capacity, clock frequency, and precision. That is why we adopted the PocketBeagle instead of the BBB for our system implementation.

Figure 10 shows the block diagram of our prototype, indicating how we have modified the firmware and hardware of OpenVLC 1.3 to implement the proposed dimming technique. As depicted, the main modifications with respect to OpenVLC 1.3 are: (i) using the PocketBeagle instead of the BBB, (ii) using different pins (General Purpose Inputs Outputs (GPIOs) and Serial Peripheral Interface (SPI)) to match with the new control board, which means (iii) modifying the firmware code for transmission and reception and the pin configuration files, and (iv) adding a new branch to the PCB cape to include the IR LED. Also, as depicted in Fig. 10, to keep the migration from BBB to PocketBeagle straightforward, we use Debian 9.2, which allows employing the same pin configuration style as for OpenVLC 1.3 and avoids issues in the driver's compilation. All the details can be found in our GitHub repository, where we make our code and hardware publicly available.

The firmware for transmission is designed to be running at the Programmable Real-time Unit 0 (PRU0) of the PocketBea-

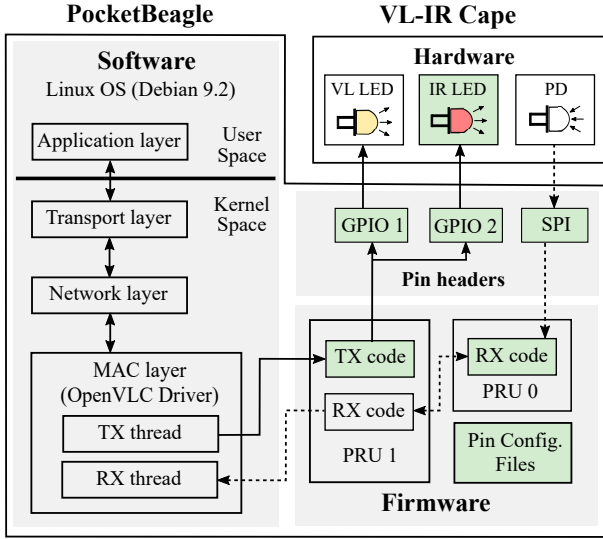


Figure 10: Block diagram of the modified version of OpenVLC 1.3 to implement our proposal. The green blocks indicate where the new changes have been introduced.

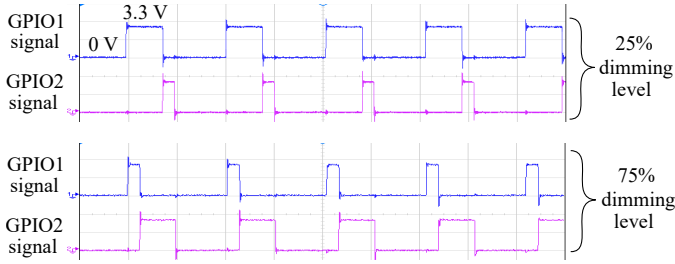


Figure 11: Oscilloscope screenshot of signals transmitted through PocketBeagle's GPIO1 (VL LED) and GPIO2 (IR LED) for dimming levels of 25% and 75%.

gle and it has three main functionalities: (1) generate the modulating signal to the selected LED (the OOK signal in Fig. 2), (2) create the PWM signal whose duty cycle (d_{PWM}) determines when to switch between the VL and IR bands and thus the provided dimming level, and (3) switch between the VL and IR LEDs by enabling the proper GPIO to control each of them. Note that the MOSFET enabling each LED is managed by a different GPIO. Also, note that our approach is easily implemented by including an additional line of code in the firmware of OpenVLC to enable/disable B1 and B2 pins depending on the configured duty cycle (illuminance). Then, the prototyping complexity is similar to a system that uses a single LED for transmission. Figure 11 shows a sample of the actual signals transmitted through GPIO1 and GPIO2 to control the VL and IR LEDs, respectively, when providing communication at dimming levels of 25% and 75%.

Figure 12 represents the schematics of the designed transmitter and how it interfaces with the GPIOs of the PocketBeagle. One important change in the transmitter hardware regarding OpenVLC 1.3 is that now we use a 12V input instead of 5V. This is because the most power-consuming components (LED and IR) operate at nearly 12V, so it reduces the stress on the voltage regulator and hence improves the thermal characteris-

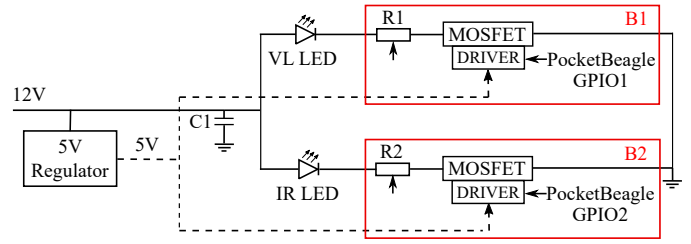


Figure 12: Schematics of the designed transmitter.

Table 4: Key components of the implemented LiFi transmitter and receiver

Component	Name
5V Regulator	LM340T-5.0
C1	0.1 μ F
VL LED	XHP35B-00-0000-0D0HC40E7
IR LED	LZ4-00R608-0000
R1, R2	3299W-1-500LF
PD	VTP4085H
MOSFET	SQ2308CES-T1_GE3
DRIVER	LM5114BMF/NOPBCT

tics of the design. The implemented prototype is shown in Fig. 9 and the key components used for the PCB implementation are summarized in Table 4. Note that our system can be used with different VL/IR LED models. We just need to adjust the output voltage of the voltage regulator (by changing the value of R1 and R2 in Fig. 12) as per the forward voltage of the VL/IR LED selected. The cost of our prototype is about 63 €, including the PocketBeagle board (35 €) and the electronic components listed in Table 4 (~ 28 €).

6.2. Experimental results

We experimentally evaluate the proposed system using the setup shown in Fig. 9b.

Figure 13 shows the illuminance received with our system at different distances and dimming levels. These experimental results show that our solution can provide a wide range of illuminance values, as represented in Fig. 13. Note that only one VL LED and one IR LED have been installed, but larger distances can be achieved if the PCB is provided with more powerful LEDs or a larger array of LEDs. To make a fair comparison, we adjust the potentiometers R1 and R2 in Fig. 12 to ensure the same amount of received power in the VL and IR spectra.

Fig. 14 represents the experimental results of UDP throughput and packet loss ratio for two different distances $D = 0.6$ m and $D = 1.2$ m, and for different dimming levels. This test is done with the *iperf* command transmitting data from our LiFi transmitter to a LiFi receiver. Note that, as obtained in the simulation results, the UDP throughput achieved with a higher dimming level is larger than the one obtained with a lower dimming level, although the illuminance is lower due to the fact that the VL LED is OFF during a time period longer than the IR LED. For example, at a distance of 1.2 m, the 100% dimming level provides the maximum UDP throughput of the OpenVLC platform (400 kb/s), whereas 0 kb/s is obtained when only the VL

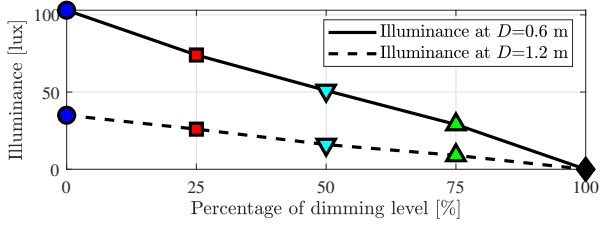
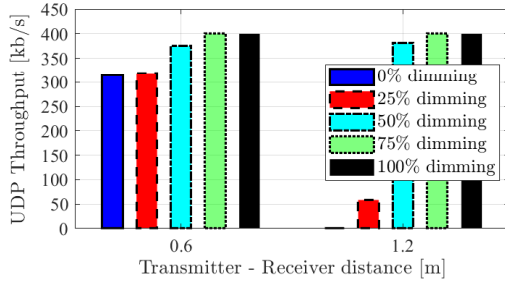
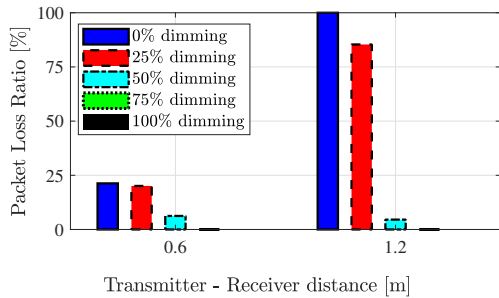


Figure 13: Illuminance for different dimming levels and distances.



(a) UDP throughput results.



(b) Packet loss ratio results.

Figure 14: Experimental results.

LED is ON, i.e., with 0% of dimming. This is because, as discussed in Section 4, photosensitive devices provide better performance when operating in the IR band. A similar effect happens with the packet loss ratio metric, i.e., the larger the dimming level, the lower the packets lost, leading to a larger UDP throughput. Note that our prototype has not been optimized to ensure a large communication range. But it can be easily done by using more powerful LEDs, an array of them, or installing optical elements such as collimators to concentrate the emitted power on a specific angle, as done in [12]. Finally, larger data rates could be achieved with a more complex hardware design, such as one based on FPGA. However, the comparison between the under-discussion techniques would be relatively equal.

We also compare the performance of our proposed solution against the case where IR and VL LEDs are decoupled for communication and illumination purposes, respectively. If LEDs are decoupled, we increase very much the power consumed per bit, as VL LED is uniquely dedicated to illumination (and

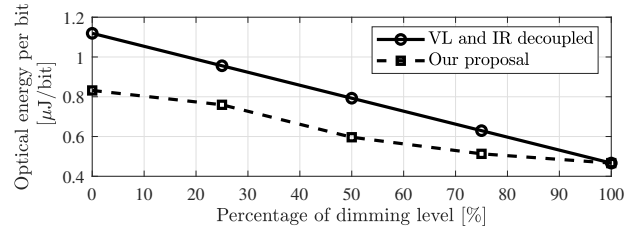


Figure 15: Optical energy per bit transmitted for each dimming level when the VL and IR LEDs are decoupled. Distance between transmitter and receiver is 0.6 m.

its energy is not used for communication) while IR LED is in charge of communication. Fig. 15 shows the results of optical energy per bit for both cases. Note that, the larger the dimming level, the lower the optical power per bit due to the increased achieved throughput. For the case where both LEDs are decoupled, the achieved UDP throughput is assumed to be the maximum allowed by the platform (400 kb/s), but the extra power consumed by the VL LED increases the optical energy per bit transmitted, achieving consumptions that are around 30% larger than the ones obtained with our proposed system.

7. Applications

Due to its low-cost, simplicity and small form factor, our system can be used in the following IoT applications:

Smart homes and offices. For these scenarios, our system allows users to easily adjust the illumination conditions in the room according to their comfort and the type of activity they are performing (sleeping, watching TV, cooking, having a meeting, projecting slides, etc.) without affecting the performance of the LiFi link to the deployed IoT devices (gadgets, smart TVs, sensors, actuators, etc.).

Indoor precision agriculture. Some recent works are promoting the use of LiFi technology to enable precision agriculture in indoor agri-food facilities (in vertical farms and greenhouses) [27]. The idea is to deploy a network of LiFi-enabled IoT devices that can sense ambient parameters such as temperature, soil moisture, humidity, etc., and to actuate accordingly over control systems such as irrigation, temperature control, etc. In such a scenario, our system (i) enables precise illumination control, which is a key factor in ensuring good-quality crops, and (ii) keeps good link performance with the LiFi IoT devices even under extremely low illumination conditions. Moreover, the ability of our system to transmit in the IR band can be leveraged as a heating source for the plants. Some works have already shown the effect of IR emissions in plant stretching or how it can positively influence germination and the total length of seeds [28]. Finally, our system can also support the deployment of in situ soil nitrate sensors that need an IR source to work [29]. By doing so, it can help to analyze soil nitrate and then optimize the fertilizer application rates in indoor agri-food facilities.

8. Conclusion

In this paper, we have proposed a fine-grained and low-power dimming scheme for joint illumination and communication using VL and IR spectra. We have validated our proposal with simulations and experimental results, and both show that it provides better communication performance than the state-of-the-art techniques under different dimming conditions. We have designed and implemented a new PCB integrating the suggested approach and extending the functionalities of the OpenVLC platform while adapting its firmware to operate with the tiny PocketBeagle, then reducing its total size, cost and power consumption. We make the software and hardware of the proposal publicly available.

Acknowledgements

This work has been partially funded by European Union's Horizon 2020 Marie Skłodowska Curie grant ENLIGHT'EM (814215), in part by the MSCA Postdoctoral Fellowship grant RISA-VLC (101061853), and in part by the project RISC-6G, reference TSI-063000-2021-59, granted by the Ministry of Economic Affairs and Digital Transformation and the European Union-NextGenerationEU through the UNICO-5G R&D Program of the Spanish Recovery, Transformation and Resilience Plan.

References

- [1] B. G. Guzman, M. S. Mir, D. F. Fonseca, A. Galisteo, Q. Wang, D. Giustiniano, Prototyping Visible Light Communication for the Internet of Things Using OpenVLC, *IEEE Communications Magazine* 61 (5) (2023) 122–128. doi:10.1109/MCOM.001.2200642.
- [2] M. S. Mir, et al., Non-Linearity of LEDs for VLC IoT Applications, in: *Proc. of the Workshop on Light Up the IoT, LIOT '20*, ACM, NY, USA, 2020, p. 6–11. doi:10.1145/3412449.3412552.
- [3] IEEE 802.15.7-2011 - IEEE Standard for Local and Metropolitan Area Networks—Part 15.7: Short-Range Wireless Optical Communication Using Visible Light. URL https://standards.ieee.org/standard/802_15_7-2011.html
- [4] IEEE 802.15.13 Task Group - Multi-Gigabit/s Optical Wireless Communications. URL <https://www.ieee802.org/15/pub/TG13.html>
- [5] IEEE P802.11 - Light Communication Task Group. URL https://www.ieee802.org/11/Reports/tgbb_update.htm
- [6] B. Agarwal, M. A. Togou, M. Marco, G.-M. Muntean, A Comprehensive Survey on Radio Resource Management in 5G HetNets: Current Solutions, Future Trends and Open Issues, *IEEE Communications Surveys & Tutorials* 24 (4) (2022) 2495–2534. doi:10.1109/COMST.2022.3207967.
- [7] X. Wu, M. D. Soltani, L. Zhou, M. Safari, H. Haas, Hybrid LiFi and WiFi Networks: A Survey, *IEEE Communications Surveys & Tutorials* 23 (2) (2021) 1398–1420. doi:10.1109/COMST.2021.3058296.
- [8] C. Mas-Machuca, M. Kaufmann, J.-P. Linnartz, M. Riegel, D. Schulz, V. Jungnickel, Techno-economic study of very dense optical wireless access using visible or infrared light, *Journal of Optical Communications and Networking* 15 (5) (2023) B33–B41. doi:10.1364/JOCN.482707.
- [9] R. Raj, et al., Dimming-Based Modulation Schemes for Visible Light Communication: Spectral Analysis and ISI Mitigation, *IEEE Open Journal of the Communications Society* 2 (2021) 1777–1798. doi:10.1109/OJCOMS.2021.3098105.
- [10] PocketBeagle, PocketBeagle board. URL <https://beagleboard.org/pocket>
- [11] D. F. Fonseca, M. S. Mir, B. G. Guzman, D. Giustiniano, Visible light or infrared? Modulating LiFi for dual operation in the visible and infrared spectra, in: *2023 18th Wireless On-Demand Network Systems and Services Conference (WONS)*, 2023, pp. 47–50. doi:10.23919/WONS57325.2023.10061923.
- [12] A. Galisteo, D. Juara, D. Giustiniano, Research in visible light communication systems with OpenVLC1.3, in: *Proc. IEEE World Forum on IoT*, 2019, pp. 539–544. doi:10.1109/WF-IoT.2019.8767252.
- [13] F. Zafar, et al., Dimming schemes for visible light communication: the state of research, *IEEE Wireless Communications* 22 (2) (2015) 29–35. doi:10.1109/MWC.2015.7096282.
- [14] T. Wang, et al., Dimming Techniques of Visible Light Communications for Human-Centric Illumination Networks: State-of-the-Art, Challenges, and Trends, *IEEE Wireless Communications* 27 (4) (2020) 88–95. doi:10.1109/MWC.001.1900388.
- [15] S. Li, et al., Unidirectional Visible Light Communication and Illumination With LEDs, *IEEE Sensors J.* 16 (23) (2016) 8617–8626. doi:10.1109/JSEN.2016.2614968.
- [16] H. Elgala, T. D. C. Little, Reverse polarity optical-OFDM (RPO-OFDM): dimming compatible OFDM for gigabit VLC links, *Optics Express* 21 (20) (2013) 24288–24299. doi:10.1364/OE.21.024288. URL <https://opg.optica.org/oe/abstract.cfm?URI=oe-21-20-24288>
- [17] Z. Tian, et al., The DarkLight Rises: Visible Light Communication in the Dark, in: *Proc. MobiCom '16*, ACM, NY, USA, 2016, p. 2–15. doi:10.1145/2973750.2973772.
- [18] T. Wang, F. Yang, C. Pan, L. Cheng, J. Song, Spectral-Efficient Hybrid Dimming Scheme for Indoor Visible Light Communication: A Subcarrier Index Modulation Based Approach, *Journal of Lightwave Technology* 37 (23) (2019) 5756–5765. doi:10.1109/JLT.2019.2938237.
- [19] Y. Yang, et al., Spatial dimming scheme for optical OFDM based visible light communication, *Optics Express* 24 (26) (2016) 30254–30263. doi:10.1364/OE.24.030254.
- [20] Z. Ghassemlooy, W. Popoola, S. Rajbhandari, *Optical Wireless Communications: System and Channel Modelling with MATLAB*, CRC Press, 2019.
- [21] B. Genoves Guzman, V. P. Gil Jimenez, DCO-OFDM Signals With Derated Power for Visible Light Communications Using an Optimized Adaptive Network-Based Fuzzy Inference System, *IEEE Transactions on Communications* 65 (10) (2017) 4371–4381. doi:10.1109/TCOMM.2017.2722477.
- [22] M. D. Soltani, A. A. Purwita, Z. Zeng, H. Haas, M. Safari, Modeling the Random Orientation of Mobile Devices: Measurement, Analysis and LiFi Use Case, *IEEE Transactions on Communications* 67 (3) (2019) 2157–2172. doi:10.1109/TCOMM.2018.2882213.
- [23] B. Genovés Guzmán, V. P. Gil Jiménez, M. C. Aguayo-Torres, H. Haas, L. Hanzo, Downlink Performance of Optical OFDM in Outdoor Visible Light Communication, *IEEE Access* 6 (2018) 76854–76866. doi:10.1109/ACCESS.2018.2882919.
- [24] J.-B. Wang, Q.-S. Hu, J. Wang, M. Chen, J.-Y. Wang, Tight Bounds on Channel Capacity for Dimmable Visible Light Communications, *Journal of Lightwave Technology* 31 (23) (2013) 3771–3779. doi:10.1109/JLT.2013.2286088.
- [25] ISO 8995:2002 Lighting of indoor work places, Standard, International Organization for Standardization, Geneva, CH (Mar. 2002).
- [26] B. Black, BeagleBone Black board. URL <https://beagleboard.org/black>
- [27] B. G. Guzman, J. Talavante, D. F. Fonseca, M. S. Mir, D. Giustiniano, K. Obraczka, M. E. Loik, S. Childress, D. G. Wong, Toward Sustainable Greenhouses Using Battery-Free LiFi-Enabled Internet of Things, *IEEE Communications Magazine* 61 (5) (2023) 129–135. doi:10.1109/MCOM.001.2200489.
- [28] M. Hernandez-Vizuet, A. Michtchenko, O. Budagovskaya, Modification of the germination and the total length of wheat seedling by an infrared-continuous wave semiconductor laser, in: *2012 9th International Conference on Electrical Engineering, Computing Science and Automatic Control (CCE)*, 2012, pp. 1–3. doi:10.1109/ICEEE.2012.6421174.
- [29] B. Gao, A. C. Walhof, D. A. Laird, F. Toor, J. P. Prineas, Analytical Evaluation of Mobile In Situ Soil Nitrate Infrared Sensor Designs for Precision Agriculture, *IEEE Sensors Journal* 21 (18) (2021) 20200–20209. doi:10.1109/JSEN.2021.3096856.